Variation of Gravity Anomaly in Ayegbami Area of Ibeju-Lekki South-West Nigeria: A Reconnaissance Geophysical Survey for Proposed Road Construction Project

Ishola S. A

Department of Earth Sciences, Olabisi Onabanjo University Ago-Iwoye, P.M.B 2002, Ago-Iwoye, Ogun State, Nigeria

Corresponding Author: *ishola.sakirudeen@oouagoiwoye.edu.ng

Abstract: *Gravity method of geophysical investigation was utilized in acquiring gravity anomaly data aimed at investigating subsurface geological conditions for proposed road construction project in Ayegami area of Ibeju Lekki, South-West Nigeria. CG-5 Autograv meter and accompanied accessories were used for the acquisition of data in two traverses with four (4) cycles each adopted for four minutes to achieve for different readings which were indicated as N1, N2, N3 and N4 where the end of N4 assigned as the last reading taken at the base station. The first reading was taken at the base station and at one-hour interval, then another reading was taken at the base station and also consecutive readings were taken from different points at every 5m distance in a traverse line against time. The data were inputted in Microsoft Excel format and consequently processed, plotted and interpreted. The bouguer and residual anomaly plots were used to indicate locations of low and high gravity anomaly along the two (2) traverses which were used for the ascertaining the locations of high and low densities and their corresponding subsurface litho-structures. Gravity changes were observed at different lateral extent at each base station. The gravity profile yielded results that reveal bouguer gravity anomalies with magnitude ranging from 188.1 to 23755 mGal. Station 3 in line N1 exhibited highest gravity values of 23755.7 mGal while station 5 in line N2 exhibited lowest gravity value of 188.1 in the entire investigated area. The change in gravity value at different station is a reflection of the status of subsurface structures. The residual anomaly profiles revealed the major anomalous regions which occurred at lateral distance between 92m to 100m with exhibited gravity value of -800000 mGal in traverse 1. Also, at lateral distance between 0m to 20m and 24m to 64m exhibited gravity values of 4400m and -6000 mGal were respectively observed. The detected and delineated anomalous zones were indicative of low-density body that could possibly represent the presence of metallic deposits/buried utilities; are of low strength could cause road failure in the area except appropriate geotechnical measures are integrated on the subsurface materials in the area of compaction and stabilization.*

Keywords: bouguer, litho-structures, compaction, cycle, reconnaissance, anomalies

INTRODUCTION

Road transportation is of great significance in any society. It predicts the state of socio-economic development in every nation of the world; no economy can thrive in the absence of road network. Road networks play notable roles to the increase of any nation gross domestic product. There are positive correlations that exist between a country's economic growth and standard of its road network. A country roads network should be designed and constructed in a systematic manner that intended social cultural and the economic benefits can be maximized (Ighodalo, 2009). It is of great significance to highlight that Nigeria roads have often being characterized with long cracks, potholes and other pavement defects. These have posed serious challenges and disaster such that in Nigeria one can hardly travel a kilometer without coming across a long cracks and potholes which has resulted to a spike in the number of road accidents and plunge on the nation's economic development. Every single road built are often known to have a stipulated design life; but roads oftentimes fail long before the planned expected date; some fail after construction, some after flooding while others last to its entire life expectancy with appropriate maintenance which necessitates the need for a preliminary investigation for a proposed road construction in the study area. The inseparable duo of Highway pavements and foundation soils toward the development of any country cannot be overemphasized (Meshida, 2006; Olofinyo et al., 2019). Diverse road failure components are observable within a short period of time after commissioning. Roads are literally constructed on geologic materials and their functioning as transport medium are impacted by the properties of these material (Gupta and Gupta, 2003; Olofinyo et al., 2019). Poor design and substandard construction activities arising from non-compliance with the recommended standards have led to loss of lives and properties. However road failures are usually accompanied by certain notable signs like such as rutting, potholes, differential heave, deformation, peeling and cracking (Alexander and Maxwell, 1996). There are several factors attributable to the increasing recorded road failures include geological, geomorphological, geotechnical factors, design and construction inadequacies, maintenances and road usage (Oke et al., 2009; Nwankwoala et al., 2014). Climatic factors in particular temperatures and attacks by acid rain have been reported to reduce the performance of the road base materials. Specifically, several pavement failures in the southern region and Niger Delta region of Nigeria have been traced to hydrogeological and geological conditions linked with swampy, textural properties of the subsoils and poor drainage measures (Jegede, 1997; Aham et al., 2005). Past investigations have also emphasized the role of geophysical in the investigation of significant factors responsible for ceaseless road failures in parts of southern Nigeria (Salami et al., 2012; Adeyemi, 2013). Ayegbami Area 1 is one of the notable areas that that can serve as feeder road to popular Lekki-Ajah-Epe express broad which makes it a potential site for proposed road construction. The road after construction is an access route linking Dangote refinery at Epe. The congested states of the aforementioned express road have slowed down the pace of socio-economic development and commercial activities in and around the area and its suburbs. The gravity method is a fundamental geophysical technique used for exploring and characterizing subsurface structures, particularly in mineral and petroleum exploration (Telford et al., 1990). It involves measuring the variations in the Earth's gravitational field, which can be caused by differences in density between subsurface rocks and minerals (Lowrie, 2007). These density variations can be indicative of subsurface geological structures, such as faults, fractures, and mineral deposits.

The application of gravity can powerfully lead to a better detection and geological interpretation of subsurface structural features and has the potential of constraining quantitative details and reducing the

ambiguity of geological interpretation. The effectiveness of gravity survey depends on the existence of a significant density contrast between altered rocks or structures and their host rocks. Gravity method is a non-destructive geophysical method that measures the difference in the Earth's gravitational field at definite locations. Gravity surveys can be carried out on the earth's surface as ground gravity survey, in the air, which is known as "aero- or airborne-gravity survey", or at sea as "marine gravity survey".

Gravity anomalies can be caused by various subsurface features such as density variations (Differences in rock density, such as between sedimentary and basement rocks), Structural features such as faults, folds, and fractures that disrupt the subsurface density distribution. Mineral deposits and Underground cavities such as empty spaces like caves, tunnels, or voids can also cause gravity anomalies. The purpose of gravity data study is to locate and describe subsurface structures from the observed gravity effects caused by their anomalous densities (Telford *et al*. 1990; Lowrie 2007).Other applications include environmental and engineering investigations, among others, Gravity interpretations are aimed at delineating the subsurface litho-structures and other features such as amplitude, shape, density contrast, frequency and closure of the gravity anomalies from bouguer anomaly, residual and regional maps/profiles and numerous enhancement maps.(Okpoli *et al*, 2019). The objective of this study is to determine the area of gravity anomaly due to low density characterization as a predictive measure of geophysical prospecting so as to ascertain the suitability of the area for the proposed road project because low density value is a potentially responsible factor to the persistence incidence of road failure (Olofinyo *et al.,* 2019).

Study Area

Location and Accessibility
The study area is the Aiyegbami area 1 of Ibeju-Lekki,Southwest Nigeria(Figure 1.1) within the Dahomey Basin. It is located between Longitude 3°52'31"to 3°52'32 East and Latitude 6°26'33"to 6°26'29"North.The study area has a gentle topography, with elevations ranging from 50 to 200 meters above sea level. The study area is accessible by road, with major roads connecting to nearby towns and cities. The terrain is relatively flat, making it suitable for gravity surveying (Figure 3.3).
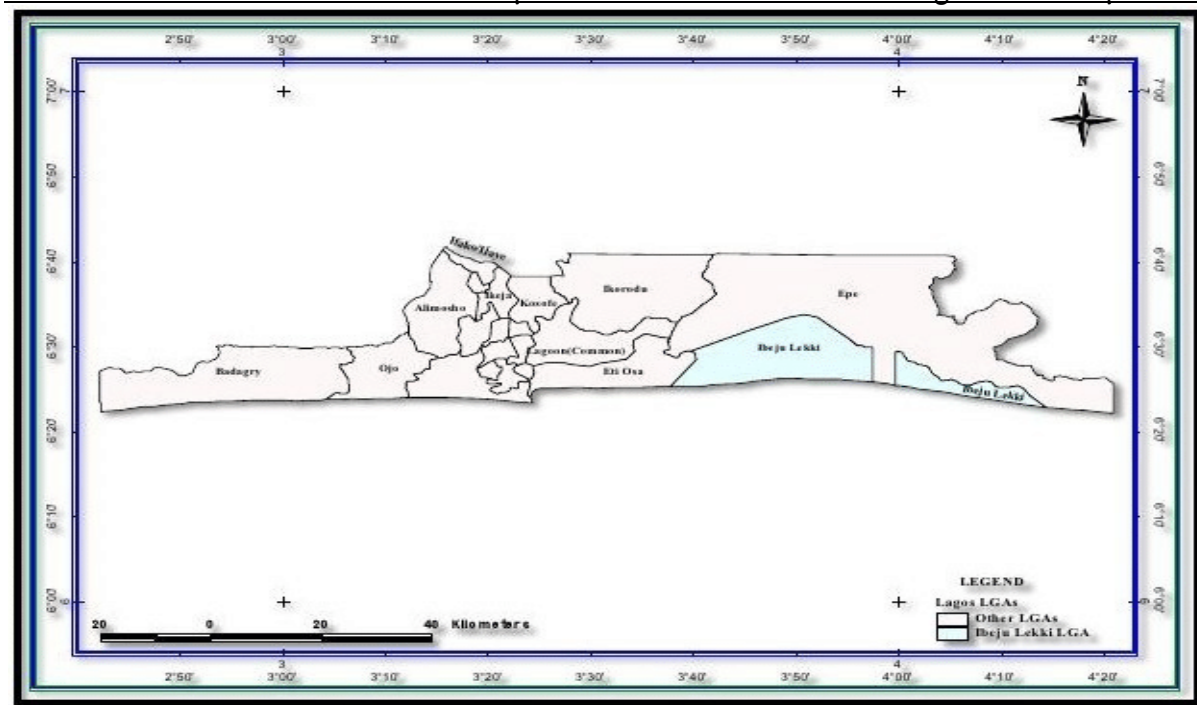
Fig. 1.1: Geographical Map of Lagos State showing Ibeju-Lekki

Relief and Drainage

The relief of the study area is very unique having both gentle and steep slope, and is made up of coastal plains, lagoon, water bodies, sand dunes, elevated areas and flood plains. The study area is drained by several rivers and streams, including the Osolo River and its tributaries. The drainage pattern is dendritic, with streams flowing into larger rivers.The area's drainage system is characterized by slow-moving rivers and streams, with minimal flooding.

Climate and Vegetation

Located at an elevation of 0 meters (0 feet) above sea level, Ibeju−Lekki experiences a tropical monsoon climate, characterized by two distinct seasons. The wet season, from April to October, brings high rainfall, high humidity, and warm temperatures. In contrast, the dry season, from November to March, is marked by low rainfall, low humidity, and warm temperatures. The area receives an average annual rainfall of 1800-2000 mm, with temperatures ranging from 22-32°C and relative humidity between 60-90%. Ibeju Lekki is situated within the tropical rainforest ecosystem, featuring diverse vegetation types. The area boasts primary rainforest, secondary rainforest, swamp forest, and mangrove forest.

Geology of the Study Area

Ibeju Lekki covers 445km^2 which equals 25% of the total landmass of Lagos state. It falls between longitudes 3°35'N and 3°55'N and Latitudes 6°25'E and 6°45'E in the creek zone of tropical Southwestern Nigeria. The area is relatively flat with an altitude of about 6.40m. It is bounded by the north by Lagos and Lekki lagoons, and to the south by the Atlantic Ocean The area of Lekki and its environs constitute part of the extensive barrier-lagoon complex in the costal margin of Southwestern Nigeria. This barrier-lagoon system is composed of five physiographic units which are broadly equivalent to sedimentary sub-environments. The units are beaches and small barrier islands, channels and creeks, open lagoons, small deltas built into lagoons, and swamps bordering the lagoons. The climate of the study area is tropical wet and dry seasons. Two dry seasons are also experienced annually, with the major dry season varying from February to April and minor dry spells varying between 20° and 37°C. February to April is the major month with peak temperature records in the study area. The relative humidity is persistently high and rarely below 70 percent throughout the year along the Lagos coast. The regional geology of Nigeria is embedded within the Pan-African mobile belt. This belt is believed to have separated Congo from West Africa Cratons (Adagunodo *et al.,* 2018). It forms part of the Lagos Lagoon system known as the largest of the four Lagoon systems of the Gulf of Guinea Coast (Adepelumi and Olorunfemi, 2000). Geologically, the study area is a sedimentary basin that falls within the coastal plain sands of the Benin Formation, which was overlain by alluvial deposits. Stratigraphy of the eastern Benin basin has been discussed by various workers and several classification schemes have been proposed. These notably include those of Jones and Hockey (1964); Omatsola and Adegoke (1981) and Billman (1992). Deposition of the Cretaceous sequence in the eastern Dahomey basin began with the Abeokuta Group, consisting of the Ise, Afowo, and Araromi Formations. Tertiary sequence includes Ewekoro, Akinbo, Oshosun, Ilaro, and coastal plain sands (Benin) Formations (Omatsola and Adegoke, 1981). The Quaternary sequence in the Dahomey basin is the Coastal Plain Sands and recent littoral alluvium which consists of poorly sorted sands with lenses of clays. The sands are in parts cross-bedded and display continental characteristics (Durotoye, 1975). However, litho-stratigraphic information from boreholes in and around Lekki-Ikoyi area reveals that typical stratigraphy sections consist of unconsolidated dry and wet sand and organic clay deposits. The deposits are sometimes inter-bedded in places with sandy-clay or clayey sand and mud with occasional varying proportion of vegetable remains and peat. The environment of deposition of these sediments was suggested to be near-shore littoral and lagoon (Longe *et al,* 1987). Within the Dahomey basin, the shallow coastal aquifer is vulnerable to climate change's impact on groundwater quality. Analysis of imagery from Google Earth and other sources has revealed shoreline changes and coastal erosion in the area. Ibeju-lekki has significant groundwater resources stored in shallow and deep aquifers (Figure 2.6).

MATERIALS AND METHODS

Theoretical Background

In any point on the earth, gravity acts in a direction normal to a surface on which the potential of gravity is constant. This equipotential surface is the best-fitting geometric figure to mean sea-level on the earth. Its shape is that of a slightly flattened spheroid for which the radius at any point can be computed. The potential gravity on this spheroid called geopotential is computed by combining the gravitational potential and the potential of the centrifugal acceleration due to earth's rotation. Gravity measurements are conducted with a high degree of accuracy and similar accuracy must be attained in order to compute a theoretical value of gravity for comparison at any latitude. Therefore, each step in computing the formula for the reference gravity must be consequently carried out to second order in the flattening f and related parameters.

When considering the ellipticity of the earth's figure, it is significant for every cros-section of earth's spheroidal shape that includes both poles to be an identical ellipse with equatorial semi-major axis a and polar semi-minor axis c which are related by flattening f through the equation

$$c = a(1-f)..3.1$$

in Cartesian co-ordinates, the equation of the ellipse is

$$\frac{x^2}{a^2} = \frac{z^2}{c^2} = 1 \quad \text{...3.2}$$

Where a position on the reference spheroid is specified by the polar angle, θ and radius r defined relative to the axis of rotational symmetry and centre of the spheroid respectively (Fig 3.1). if we are to consider a polar crossection that includes the x and z axes so that $x = r \cos \theta$ by substituting into equation 3.2, we simply obtain the equation of the elliptical section in polar coordinates (Lowrie, 2011).

$$\frac{r^2 \sin^2 \theta}{a^2} + \frac{r^2 \cos^2 \theta}{c^2} \quad \text{...3.3}$$
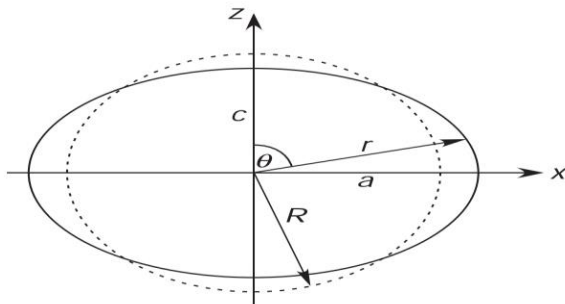

Fig. 3.1: Polar cross-section of a spheroid with principal axes a and c (c < a), compared with a sphere (dashed) with radius R and the same volume as spheroid (Lowrie, 2011).

$$\frac{r^2}{a^2} \left(\sin^2 \theta + \frac{\cos^2 \theta}{(1-f)^2}\right) = 1 \quad \text{..3.4}$$

Slight rearrangement turned equation 3.4 to equation 3.5 where

$$r^2 = \frac{a^2(1-f)^2}{\cos^2\theta + (1-f)\sin^2\theta^2} \quad \dots\dots\dots\dots\dots\dots\dots\dots\dots\dots\dots\dots\dots\dots\dots.3.5$$

The expansion of the denominator in equation 3.5 gives

$$\cos^2\theta + (1-f)\sin^2\theta^2$$
$$= (1-2f+f^2)\sin^2\theta + \cos^2\theta$$
$$= \sin^2\theta + \cos^2\theta - 2f\sin^2\theta + f^2\sin^2\theta \quad \dots\dots\dots\dots\dots\dots\dots\dots\dots..3.6$$

It is worthy of note that $\sin^2\theta + \cos^2\theta = 1$. Thus, equation 3.6 can be re-written as

$$= 1 - 2f\sin^2\theta + f^2\sin^2\theta(1)$$
$$= 1 - 2f\sin^2\theta + f^2\sin^2\theta(\sin^2\theta + \cos^2\theta)$$
$$= 1 - 2f\sin^2\theta + f^2\sin^4\theta + f^2\sin^2\theta\cos^2\theta)$$
$$= (1 - f\sin^2\theta)^2 + f^2\sin^2\theta\cos^2\theta) \quad \dots\dots\dots\dots\dots\dots\dots\dots\dots..3.7$$

By substituting this back to equation 3.5 and taking the square root afterwards, we obtain a representative equation for radius

$$r^2 = \frac{a^2(1-f)^2}{\sqrt{(1-f\sin^2\theta)^2 + f^2\sin^2\theta\cos^2\theta)}}$$
$$\frac{r}{a} = \frac{1-f}{((1-f\sin^2\theta)^2 + f^2\sin^2\theta\cos^2\theta))^{\frac{1}{2}}}$$
$$\frac{r}{a} = \frac{1-f}{1-f\sin^2\theta}\left(1 + \langle\frac{f^2\sin^2\theta\cos^2\theta}{(1-f\sin^2\theta)^2}\rangle\right)^{\frac{-1}{2}} \quad \dots\dots\dots\dots\dots\dots\dots\dots..3.8$$

Applying the binomial theorem twice to the last line and expanding to order f^2, we obtain an equation for the surface of a spheroid.

$$\frac{r}{a} \approx \frac{1-f}{1-f\sin^2\theta}\left(1 - \frac{1}{2}f^2\sin^2\theta\cos^2\theta\right)$$
$$\frac{r}{a} \approx \frac{1-f}{1-f\sin^2\theta} \quad \dots\dots\dots\dots\dots\dots\dots\dots\dots\dots\dots\dots\dots.3.9$$

The expansions for the gravitational potential and for gravity on the reference ellipsoid require the ratio a/r. If the equation 3.9 is inverted with the aid of the binomial expansion, we simply obtain to an order f^2.

$$\frac{a}{r} \approx \frac{1-f\sin^2\theta}{1-f}\left(1 + \frac{1}{2}f^2\sin^2\theta\cos^2\theta\right)$$
$$\frac{a}{r} \approx (1 - f\sin^2\theta)(1 + \frac{1}{2}f^2\sin^2\theta\cos^2\theta)(1+f+f^2+\dots\dots)$$
$$\frac{a}{r} \approx 1 + f + f^2 - f\sin^2\theta - f^2\sin^2\theta + \frac{1}{2}f^2\sin^2\theta\cos^2\theta \quad \dots\dots\dots\dots\dots.3.10$$
$$\frac{a}{r} \approx 1 + f\cos^2\theta + f^2\cos^2\theta + \frac{1}{2}f^2\cos^2\theta - \frac{1}{2}f^2\cos^4\theta$$
$$\frac{a}{r} \approx 1 + f(1 + \frac{3}{2}f)\cos^2\theta - \frac{1}{2}f^2\cos^4\theta \dots\dots\dots\dots\dots\dots\dots\dots\dots.3.11$$

The main component of gravity is the gravitational acceleration a_G towards the centre of the earth. Gravitational acceleration varies with latitude because of the varying radius of the spheroid. The departure from a spherical shape results from the deforming effect of earth's rotation which produces a centrifugal acceleration a_C which is directed perpendicular to and away from axis of

rotation (Fig. 3.2). This component is proportional to the distance from the rotation axis, so it equally varies with latitude (Lowrie, 2011).

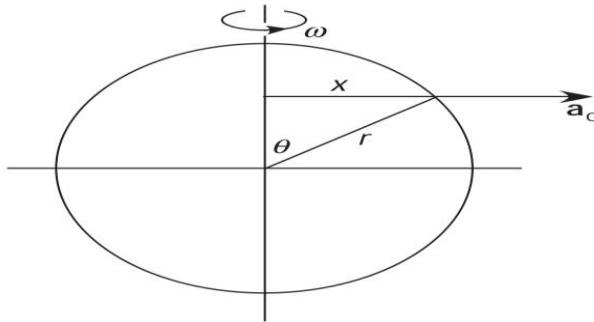Fig. 3.2: Centrifugal acceleration a_c at co-latitude θ, directed perpendicular to and away from the axis of rotation (Lowrie, 2011).

Gravity is the vector combination of the centrifugal and gravitational components each of which is conservative and is the gradient of a scalar potential. Therefore, geopotential is the potential of gravity U_g at a given point on earth's surface; it is mathematically expressed as the sum of the gravitational potential U_G and centrifugal potential U_C at that point

$U_g = U_G + U_C$ …………………………………………………3.12

The computation of gravity on the reference spheroid necessitates the derivation and determination of geopotential to second order in the small quantities that define it where each of the quantities f, m, and J_2 is around 10^{-3} in size rendering their squares and products to be around 10^{-6}. The gravitational potential must be determined with the same definition depicting that it is quite inadequate to utilize only the terms up to J_2. The term J_3 can be omitted if we assume that the mass distribution of the earth is symmetric about the equator but it is required that the term J_4 is included for an accurate description of gravitational potential up to the term J_4, U_G therefore becomes

$U_G = -\frac{GE}{a}\left[\left(\frac{a}{r}\right) - J_2\left(\frac{a}{r}\right)^3 P_2(\cos\theta) - J_4\left(\frac{a}{r}\right)^5 P_4(\cos\theta)\right]$………………………..3.13

The centrifugal acceleration a_C is the gradient of the centrifugal potential i.e

$a_C = -\nabla U_C$ …………………………………………………….3.14

Let x be the perpendicular distance from the rotation axis to a point on the surface at latitude θ and let ω be the the angular rate of rotation of the earth (Fig. 3.2). The centrifugal acceleration is equal to $\omega^2 x$. So, for a constant rate of rotation, U_C varies only with x. Therefore, the above statement is mathematically expressed as

$-\frac{\partial U_C}{\partial x} = \omega^2 x$ …………………………………………………….3.15

Integrating both sides with respect to x, we have

$U_C = -\frac{\omega^2 x^2}{2} + U_0$

$U_C = -\frac{1}{2}\omega^2 x^2 + U_0$ …………………………………………………..3.16

The implication is that the potential is zero at this axis of rotation where $x = 0$, and the constant of integration $U_C = 0$. The equation for the centrifugal potential in terms of the polar angle θ is

$$U_C = -\frac{1}{2}\,\omega^2 x^2$$

$$U_C = -\frac{1}{2}\,\omega^2 r^2 \sin^2\theta \quad\dots\dots\dots\dots\dots\dots\dots\dots\dots\dots\dots\dots\dots\dots\dots 3.17$$

The Equipotential surface of Gravity

In order to compute gravity accurately on the reference ellipsoid, it is necessary to develop the geopotential to second order in the small quantities f, m and J_2, the gravitational potential coefficient of J_4 whose magnitude is around 10^{-6} must also be utilized. The geopotential consists of the sum of the gravitational and centrifugal potentials (Lowrie, 2011).

$$U_g = -\frac{GE}{a}\left[\left(\frac{a}{r}\right) - J_2\left(\frac{a}{r}\right)^3 P_2(\cos\theta) - J_4\left(\frac{a}{r}\right)^5 P_4(\cos\theta)\right]$$

$$U_g = -\frac{1}{2}\,\omega^2 a^2 \left(\frac{r}{a}\right)^2 \sin^2\theta \quad\dots\dots\dots\dots\dots\dots\dots\dots\dots\dots\dots\dots\dots 3.18$$

Taking the centrifugal term inside the bracketed expression renders equation 3.18 to be

$$U_g = -\frac{GE}{a}\left[\left(\frac{a}{r}\right) - J_2\left(\frac{a}{r}\right)^3 P_2(\cos\theta) - J_4\left(\frac{a}{r}\right)^5 P_4(\cos\theta) + \frac{1}{2}\left(\frac{\omega^2 a^3}{GE}\right)\left(\frac{r}{a}\right)^2 \sin^2\theta\right]\dots\dots 3.19$$

The geopotential involves the ratio of $\frac{a}{r}$, $\left(\frac{a}{r}\right)^3$, and $\left(\frac{a}{r}\right)^5$ whhich we can generate from equation 3.11. It should be noted that the term $\left(\frac{a}{r}\right)^3$ is multiplied by J_2, so it must be evaluated only to first order in f; the coefficient J_4 is itself of order 10^{-4}, so the ratio $\left(\frac{a}{r}\right)^5$ on the equipotential surface of gravity may be set equal to 1. Then

$$\left(\frac{a}{r}\right) \approx 1 + 3(f(1+\tfrac{3}{2}f)\cos^2\theta - \tfrac{1}{2}f^2\cos^4\theta) \approx 1 + 3(f\cos^2\theta)\dots\dots\dots\dots\dots 3.20$$

For the purpose of succinctness and identification, let the last term in the brackets in equation 3.20 be identified as ψ. The ratio $\frac{r}{a}$ is obtained from equation 3.9. Therefore,

$$\psi = \frac{1}{2}\left(\frac{\omega^2 a^2(1-f)}{GE}\right)\frac{(1-f)\sin^2\theta}{(1-f\sin^2\theta)^2} \quad\dots\dots\dots\dots\dots\dots\dots\dots\dots\dots\dots 3.21$$

$$\psi = \frac{1}{2}\,m\,\frac{(1-f)\sin^2\theta}{(1-f\sin^2\theta)^2} \quad\dots\dots\dots\dots\dots\dots\dots\dots\dots\dots\dots\dots 3.22$$

Where m is the centrifugal acceleration ratio given as

$$m = \frac{\omega^2 a^2(1-f)}{GE} \quad\dots\dots\dots\dots\dots\dots\dots\dots\dots\dots\dots\dots\dots\dots 3.23$$

The denominator in equation 3.22 can be further expanded using binomial theorem; this is expected to be in first order only because of the factor m which is similar in size to f. The centrifugal term ψ becomes

$$\psi = \frac{1}{2}\,m\,(1-f)(1+2f\sin^2\theta)\sin^2\theta \quad\dots\dots\dots\dots\dots\dots\dots\dots 3.24$$

Determining the product of expression of equation 3.24 and retaining only the terms of first order in f given

$$\psi = \frac{1}{2}\,m\,(1-f)(1+2f\sin^2\theta)\sin^2\theta \quad\dots\dots\dots\dots\dots\dots\dots\dots 3.25$$

In the equation for the geopotential, the centrifugal term must be combined with a term in $J_2 P_2(\cos\theta)$, which has the form $(\cos^2\theta)$ and a term $J_4 P_4(\cos\theta)$, which contains terms in both $\cos^2\theta$ and $\cos^4\theta$ (Lowrie, 2011).

$$\psi = \frac{1}{2}\, m\, (1 - \cos^2\theta)(1 - f + 2f)(1 - \cos^2\theta)$$

$$= \frac{1}{2}\, m\, (1 - \cos^2\theta)(1 - f + 2f)(1 - \cos^2\theta)$$

$$= \frac{1}{2}\, m\, (1 - \cos^2\theta)(1 - f + 2f)(1 - \cos^2\theta)$$

$$= \frac{1}{2}\, m\, (1 + f - 2f\cos^2\theta - \cos^2\theta - f\cos^2\theta + 2f\cos^4\theta)\dots\dots\dots3.26$$

$$= \frac{1}{2}\, m\, (1 + f - (1 + 3f)\cos^2\theta + 2f\cos^4\theta)\dots\dots\dots\dots\dots\dots3.27$$

Returning back to equation 3.19, we can state the full expressions for $P_2(\cos\theta)$ and $P_4(\cos\theta)$ and the ratios a/r from equation 3.11 and $(a/r)^3$ from equation 3.20 and using equation 3.27 for the centrifugal term, we get the geopotential as a function of $\cos^2\theta$ and $\cos^4\theta$.

$$U_g = -\frac{GE}{a}\begin{bmatrix} 1 + (1 + \frac{3}{2}f)\cos^2\theta - \frac{1}{2}f^2\cos^4\theta \\[6pt] -J_2(-1 + 3(1 - f)\cos^2\theta + {9f\cos^4\theta}/{2} \\[6pt] -J_4(3 - 30\cos^2\theta + 35\cos^4\theta}/{8} \\[6pt] +\frac{1}{2}\, m\, (1 + f - (1 + 3f)\cos^2\theta + 2f\cos^4\theta \end{bmatrix}\dots\dots\dots\dots\dots3.28$$

After gathering terms to get the coefficients that multiply $\cos^2\theta$ and $\cos^4\theta$, we get the final expression for the geopotentials (Lowrie, 2011).

$$U_g = -\frac{GE}{a}\begin{bmatrix} 1 + f + \frac{1}{2}m + \frac{1}{2}J_2 - \frac{3}{8}J_4 \\[6pt] +(f + \frac{3}{2}f^2 - \frac{1}{2}m - \frac{3}{2}fm - \frac{3}{2}(1 - f)J_2 + \frac{15}{4}J_4)\cos^2\theta \\[6pt] -(\frac{1}{2}f^2 - mf + \frac{9}{2}fJ_2 + \frac{35}{8}J_4)\cos^4\theta \end{bmatrix}\dots\dots\dots\dots3.29$$

Though by definition, the geopotential must be constant on the equipotential surface. However, the potential in equation 3.29 can vary with polar angle through the terms in $\cos^2\theta$ and $\cos^4\theta$. This apparent contradiction implies that the coefficients of these terms must be zero.

Gravity Field and Anomalies
The gravity field is the vector sum of gravitational attraction from all subsurface masses. It is a three-dimensional field that varies in magnitude and direction with location. Gravity anomalies are variations that deviate from the expected value, caused by subsurface structures like faults, folds, density variations, underground cavities, and mineral deposit. There are several types of gravity anomalies and they include: Regional anomalies which are large-scale variations in the gravity field, often related to crustal thickness or sedimentary basin structures. Local anomalies which are smaller-scale variations, typically associated with specific subsurface features like faults, folds, or mineral deposits.Residual anomalies which are anomalies remaining after removing regional trends, highlighting local subsurface features.

Bouguer anomalies are anomalies corrected for the gravitational effect of the Earth's surface topography. Gravity anomalies can be caused by various subsurface features such as density variations (Differences in rock density, such as between sedimentary and basement rocks), Structural features such as faults, folds, and fractures that disrupt the subsurface density distribution. Mineral deposits and Underground cavities such as empty spaces like caves, tunnels, or voids can also cause gravity anomalies.

Regional and Residual Anomalies
The resultant effects of the inhomogeneous distribution of density in the Earth give rise to the development of a gravity anomaly (Lowrie, 1997). Over a high density body, the measured gravity is augmented, after reduction to the reference ellipsoid and subtraction of the normal gravity a positive gravity anomaly is obtained. Likewise, a negative anomaly results over a region of low density (Lowrie, 1997). The presence of a gravity anomaly indicates a body or structure with anomalous density; the sign of the anomaly is the same as that of the density contrast and shows whether the density of the body is higher or lower than normal. The appearance of a gravity anomaly is affected by the dimensions, density contrast and depth of the anomalous body. The horizontal extent of an anomaly is often called its apparent wavelength. The wavelength of an anomaly is a measure of the depth of the anomalous mass. Large, deep bodies give rise to broad (long-wavelength), low-amplitude anomalies while small, shallow bodies cause narrow(short-wavelength), sharp anomalies (Lowrie, 1997). Usually a map of Bouguer gravity anomalies contains superposed anomalies from several sources. The long-wavelength anomalies due to very deep density contrasts are called regional anomalies. They are important for understanding the large scale structure of the earthcrusts under major geographic features such as mountain ranges, oceanic ridges and subduction zones. Short–wavelength residual anomalies are due to shallow anomalous masses that may be of interest for commercial exploitation. Geological knowledge is essential for interpreting residual anomalies. In eroded shield area like Canada or Scandinavia, anomalies with very short wavelength may be due to near-surface mineralized bodies. In sedimentary basins, short or intermediate wavelength anomalies may arise from structures related to reservoirs or natural gas (Lowrie, 1997).

Separation of Regional and Residual Anomalies
The separation of anomalies of regional and local origin is an important step in the interpretation of a gravity map. The analysis may be used on selected profiles across some structure or it may involve two dimensional distributions of anomalies in a gravity map (Lowrie, 1997). Numerous techniques have been applied to the decomposition of a gravity anomaly into its constituent parts. They range in sophistication from simple visual inspection of the anomaly pattern to advanced mathematical analysis. A few examples are described below.

Visual Analysis
Visually fitting the large –scale trend with a smooth curve is the simplest way of representing the regional anomaly on a gravity profile (Lowrie, 1997). The value of the regional gravity given by this trend is subtracted point by point from the Bouguer gravity anomaly. This method allows the

interpreter to fit curves that leave residual anomalies with a sign appropriate to his interpretation of the density distribution. This approach may be adapted to the analysis of a gravity map by visually smoothing the contour lines (Lowrie, 1997). The values of the regional and original Bouguer gravity anomaly are interpolated from the corresponding maps at points spaced on a regular grid. The regional value is subtracted from the Bouguer anomaly at each point and the computed residuals are contoured to give a map of the local gravity anomaly.

Polynomial Representation
In an alternative method, the regional trend is represented by a straight line on more generally by smooth polynomial curve (Lowrie, 1997). If x denotes the horizontal position on a gravity profile, the regional gravity Δg_R may be written as
$$\Delta g_R = \Delta g_0 + \Delta g_1 x + \Delta g_2 x^2 + \Delta g_3 x^3 + \Delta g_4 x^4 + \Delta g_5 x^5 + \ldots + \Delta g_n x^n \ldots\ldots.3.30$$
The polynomial is fitted by the method of least squares to the observed gravity profile. This gives optimum values for the coefficients Δg_n. The method also has drawbacks. The higher the order of the polynomial, the better it fits the observations. The ludicrous extreme is when the order of the polynomial is one less than the number of observations, the curve then passes perfectly through all the data points but the regional gravity anomaly has no meaning geologically. The interpreter's judgment is important in selecting the order of the polynomial which is usually chosen to be the lowest possible order that represent most of the regional trend. Moreover, a curve fitted by least squares must pass through the mean of the gravity values so that the residual anomalies are divided equally between positive and negative values. Each residual anomaly is flanked by anomalies of opposite sign which are due to the same anomalous mass that caused the central anomaly and so have no significance of their own. Polynomial fitting can also be applied to gravity maps. It is assumed that the regional anomaly can be represented by a smooth surface, $\Delta_g (x, y)$, which is a low-order polynomial of the horizontal position coordinates $x, and\ y$. In the simplest case, the regional anomaly is expressed as a first order polynomial or plane, to express changes in the gradient of gravity; a higher-order polynomial is needed. For example, the regional gravity given by a second-order polynomial is
$$\Delta_g (x, y) = \Delta g_0 + \Delta g_{x1} x + \Delta g_{y1} y + \Delta g_{x2} x^2 + \Delta g_{y2} y^2 + \Delta g_{5xy} xy \ldots\ldots\ldots.3.31$$
As in the analysis of a profile, the optimum values of the coefficients $\Delta g_{x1}, \Delta g_{y1} y$ and others are determined by least squares fitting. The residual anomaly is again computed point by point by subtracting the regional from the original data.

Fourier Analysis
The gravity anomaly along a profile can be analyzed with techniques developed for investigating time series (Lowrie, 1997). Instead of varying with time as the seismic signal does in a seismometer, the gravity anomaly $\Delta g(x)$ varies with position x along the profile. For a spatial distribution, the wave number $k = \frac{2\pi}{\lambda}$ is the counterpart of the frequency of a time series. If it can be assumed that its variation is periodic, the function $\Delta g(x)$ can be expressed as the superposition of discrete harmonics. Each harmonic is a sine or cosine function whose argument

is a multiple of the fundamental wave number which is defined by a wavelength $\boldsymbol{\lambda}$ that is twice the signal strength of the anomaly

$$\Delta g(x) = \sum_{n=1}^{N}(a_n \cos\frac{2n\pi x}{\lambda} + b_n \sin\frac{2n\pi x}{\lambda}) \quad \dots\dots\dots\dots\dots\dots\dots\dots\dots\dots\dots\dots\dots\dots\dots.3.32$$

The expression for $\Delta g(x)$ is called Fourier series. In this example, it is truncated after N sine and N cosine terms. In principle, the value of N can be as large as necessary to describe the regional anomaly adequately, a decision is that must be made on practical grounds by the interpreter. The importance of any individual term of order n is described by the relative value of the coefficients a_n and b_n to be calculated. If integrated over a full cycle, the resulting value of a sine or cosine function is zero; only the squared values of sine or cosines do not integrate to zero. If equation 3.32 is multiplied by $\cos\frac{2m\pi x}{\lambda}$, we get $\Delta g(x)\cos\frac{2m\pi x}{\lambda}$ on the left side and product terms $\cos\frac{2n\pi x}{\lambda}\cos\frac{2m\pi x}{\lambda}$ and $\sin\frac{2n\pi x}{\lambda}\cos\frac{2m\pi x}{\lambda}$ on the right side. Each product can be written as the sum or difference of the two sines or cosines. Thus, if the $\Delta g(x)\cos\frac{2m\pi x}{\lambda}$ is integrated over a full cycle, all terms on the right side vanish except for the case where n equals m; this yields the values of the coefficients a_n and b_n, namely

$$a_n = \frac{2}{\lambda}\int_0^{\lambda}\Delta g(x)\cos\frac{2n\pi x}{\lambda}dx$$

$$b_n = \frac{2}{\lambda}\int_0^{\lambda}\Delta g(x)\sin\frac{2n\pi x}{\lambda}dx \quad \dots\dots\dots\dots\dots\dots\dots\dots\dots\dots\dots\dots\dots\dots\dots.3.33$$

The two dimensional variation of a mapped gravity anomaly can be expressed in a similar way with the aid of *double fourier series*. In this case, the gravity anomaly is a function of both the $x-$ and y –coordinates and can be written as

$$\Delta g(x,y) = \sum_{n=1}^{N}\sum_{m=1}^{M} a_{nm}C_nC_m + b_{nm}C_ns_m + c_{nm}S_nC_m + d_{nm}S_nS_m \dots\dots\dots\dots.3.34$$

Where

$$C_n = \cos\frac{2n\pi x}{\lambda}; S_n = \sin\frac{2n\pi x}{\lambda}$$

$$C_m = \cos\frac{2m\pi x}{\lambda}; S_n = \sin\frac{2m\pi y}{\lambda} \quad \dots\dots\dots\dots\dots\dots\dots\dots\dots\dots\dots\dots\dots\dots.3.35$$

The derivation of the coefficients a_{nm}, b_{nm}, c_{nm}, and d_{nm} is similar to the one-dimensional case, but is somewhat more complicated. As in the simpler one-dimensional case of gravity anomaly on a profile the expression of two dimensional gravity anomalies by double fourier series is analogous to summing weighted sinusoidal functions. These can be visualized as corrugations of the $x-y$ plane with each corrugation weighted according to its importance to $\Delta g(x,y)$.

Gravity Anomaly Enhancement and Filtering
Since a function that is periodic can be expressed as a Fourier sum of harmonics of a fundamental wavelength. The requirement of periodic behaviour and discreteness of harmonic content are often not met. For example, the variation of gravity from one point to another is usually not periodic (Lowrie, 1997). Moreover, if the harmonic content of a function is made up of distinct multiples of a fundamental frequency or wave number, the wavelength spectrum consists of a number of distinct values. Yet many functions of geophysical interest are best represented by a continuous spectrum of wavelengths. This kind of problem, fourier sum of individual terms is replaced by

fourier integral which consists of a continuous set of frequencies and wave numbers instead of a discrete set. The fourier integral can be used to represent non-periodic functions. It is uses complex numbers (numbers that involve the square root of −1). Instead of equation 3.32, we have

$$g(x) = \int_{-\infty}^{\infty} G(u) \, e^{iuxdu}$$

Where

$$G(u) = \frac{1}{2\pi} \int_{-\infty}^{\infty} \Delta g(x) \, e^{-iuxdx} \quad \dots\dots\dots\dots\dots\dots\dots\dots\dots\dots\dots 3.36$$

The complex function $G(u)$ defined by equation 3.36 is called the fourier transform of the real – valued function $\Delta g(x, y)$. A map of gravity anomalies can be represented by a function $\Delta g(x, y)$ of the Cartesian map coordinates. The fourier transform of $\Delta g(x, y)$ is a two-dimensional complex function that involves wave number k_x band k_y defined by wavelength of the gravity field with respect to the x and y axes ($k_x = 2\pi/\lambda_x$; $k_y = 2\pi/\lambda_y$). It is

$$G(x, y) = \int_{-\infty}^{\infty} \int_{-\infty}^{\infty} \Delta g(x, y) \{\cos(k_x x + k_y y) - \sin(k_x x + k_y y)\} \dots\dots\dots\dots\dots 3.36$$

This equation assumes that the observation $\Delta g(x, y)$ can be represented by a continuous function defined over an infinite $x - y$ plane whereas the data are of time extent and are known at discrete points of a measurement grid. In practice, these inconsistencies are usually not important. Efficient computer algorithms permit the rapid computation of the fourier transform $G(x, y)$ of the gravity anomaly $\Delta g(x, y)$. The two dimensional Fourier transform simplifies the operation of digital filtering the gravity anomalies. A filter is a spatial function of the coordinates x and y. When the function $\Delta g(x, y)$ representing the gravity data is multiplied by the filter function, a new function is produced. The process is called convolution and the output is a map of the filtered gravity data. The computation in the spatial domain defined by the x and y coordinates can be time consuming. It is often faster to compute the fourier transforms of the gravity and filter functions multiply these together in the fourier domain and inverse fourier transform the product back to the spatial domain. The nature of the filter applied in the fourier domain can be chosen to eliminate certain wavelengths. For example, it can be designed to cut out all wavelengths. For example, it can be designed to cut out all wavelengths shorter than a selected wavelength and to pass longer wavelengths; this is called a low pass filter because it passes long wavelengths that have low wave numbers. The irregularities in bouguer gravity anomaly map are removed by low pass filtering leaving a filtered map that is much smoother than the original. Alternatively, the filter in the fourier domain can be designed to eliminate wavelength longer than a selected wavelength and to pass shorter wavelengths. The application of such high-pass filter enhances the short-wavelengths. The application of such a high –pass filter enhances the short-wavelength (high wave number) components of the gravity map. Wavelength filtering can be used to emphasize selected anomalies. For example, in studying large−scale crustal structure the gravity anomalies due to local small bodies are of less interest than the regional anomalies which can be enhanced by applying a low pass filter. Conversely, in the investigation of anomalies due to shallow crustal sources the regional effect can be suppressed by high–pass filtering (Lowrie, 1997).

Field Operations for Data Acquisition in the Study Area

Gravity method of geophysical Investigation was utilized in Magbon-Alade to determine subsurface anomalous variation using Scintrex (CG3-M Autograv). The equipment was calibrated before working hours so that the restoring force can be translated into precise measuring of gravity, typically in units of milliGals (mGal). The equipment was placed on the tripod and leveled using the tripod screws.(Figure 3.3). A 100m long profile with a space of 5m and interpole cycle (N) of N1, N2, N3 and N4 was adopted for relatively deeper penetration. A base station was picked then different points were taken on a traverse line 5m apart and two traverse was used with 5meters spacings. Each readings takes 4 minutes and at1hours interval, a reading is being taken at the base station while GPS was used to collate the coordinate and altitude in each station. The first reading was taken at the base station and every hour, readings were taken at the base station to serve as references and to ensure standardization of gravity measurements. Consecutive readings were taken from different points at 5m distance from each other in a traverse line. Each traverse line had a 2m distance from each other. The instrument was powered on and was leveled by rotating the foot screws in the direction indicated by the icons on the top corners of the screen. The orientation is shown in arc seconds and the definition of the axes of rotation and the sign convection is shown. Rotation was continued until the intersection of the cross-hairs was within the small circle ($\pm$ 10 arcsec). After the arc of the circle was achieved, the measure button was used to process the data acquisition. The current column on the gravimeter screen contains the current gravity value after filtering and with all corrections applied together with the other measured variables, time and station information. Initially, the last recorded reading was displayed in the preceding column. In the course of this study, four cycles for four minutes were used to achieve four different readings which were indicated as N1, N2, N3, and N4 which represent gravity data or measurements at a specific location or station. N1 represents (the initial gravity measurement at a station), N2 represents (the second measurement at the same location usually taken every minute, N3 represents the third measurement and N4 represents the fourth reading. For a daily survey, the assumption of a linear drift is typically sufficient; however, as demonstrated by Bonval et*et al.,* (1998), there are noticeable changes in linearity in the recordings made over several days of continuous gravity field measurement. As a result, the user must return to the base more often than every 0.5 hr, for continuous surveys. In detail surveys one of the key parts is to remove the earth tide effect because their body gravity effects could be larger than variations in margins on a site due to changes beneath the land surface which are intended for environmental and engineering investigations. The raw data were imputed into the system in Excel format consequently processed, plotted and interpreted.

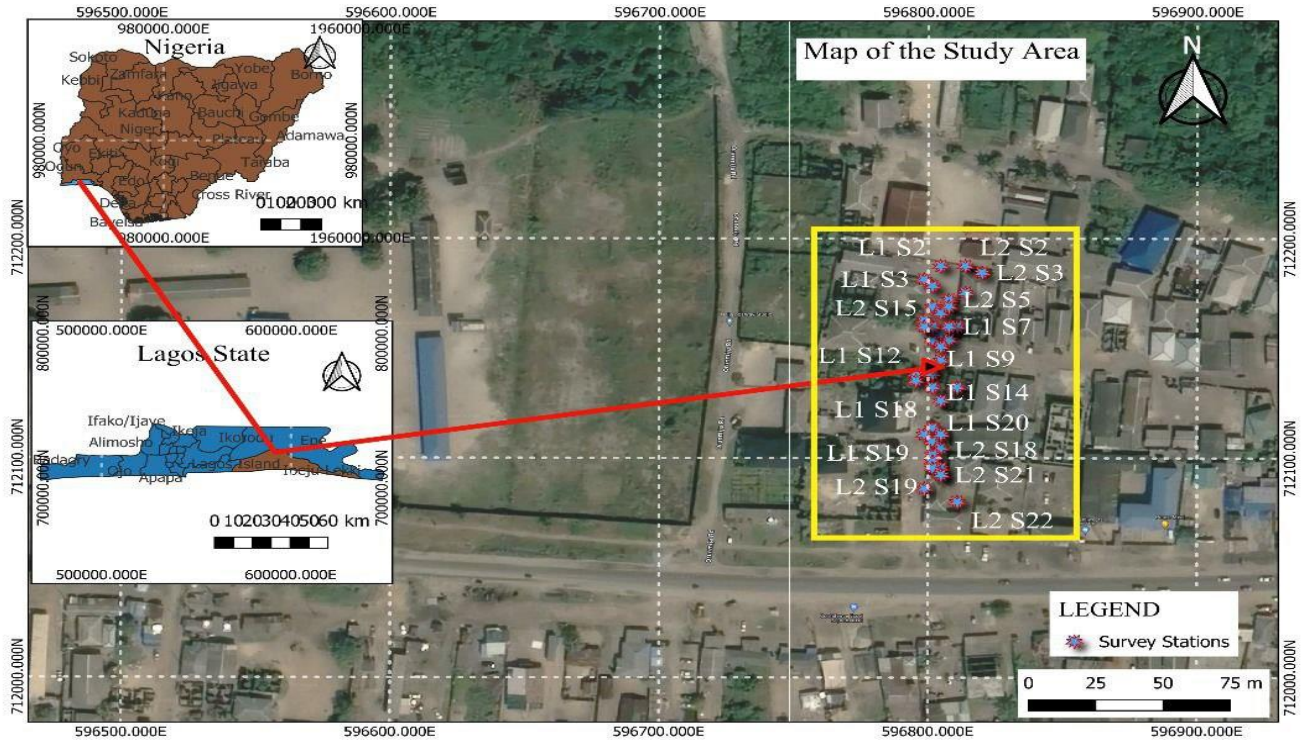Figure 3.2: A picture showing the equipment screen and other field accessories

Figure 3.3: Satellite Map of the Study Area in Google Earth Imagery

RESULTS AND DISCUSSION

Gravity Variations of the study Area

Description of Gravity Variation in Traverse 1

The variation in gravity values were observed and interpreted using 3D Stacked Column, using 3D lines, High –Low close Description as respectively displayed in figure 4.1a, 4.1b and 4.1c for traverse line 1.
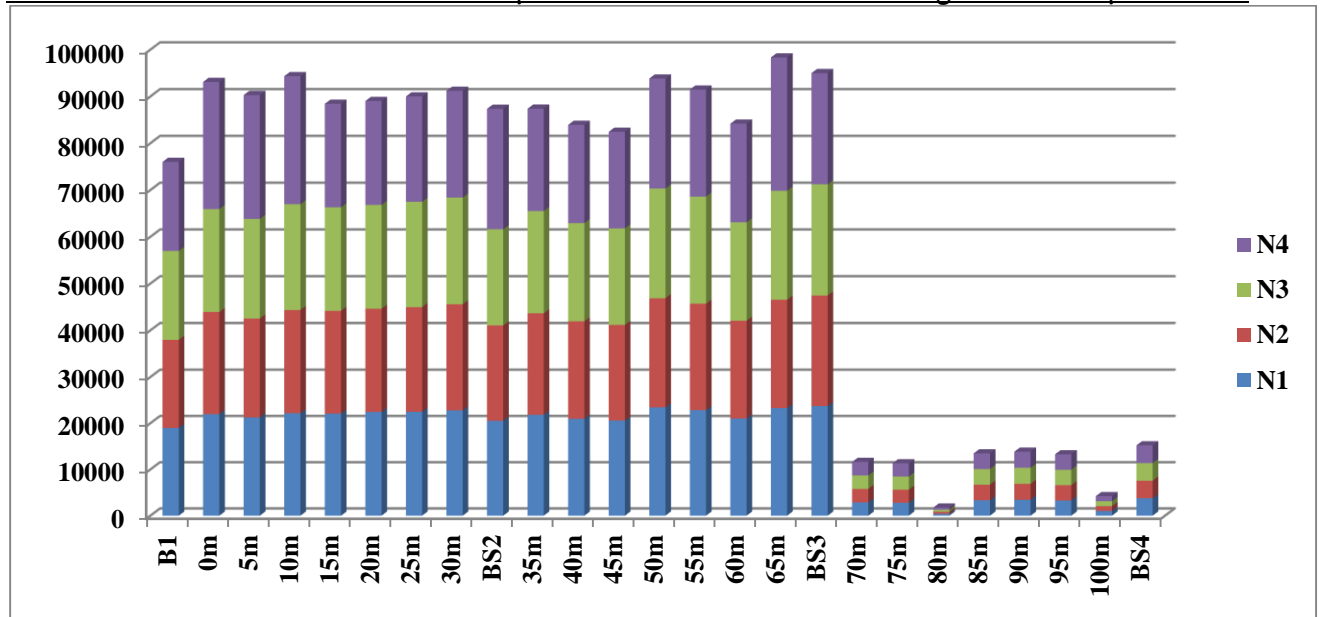
Figure 4.1a: Distribution of gravity changes in Aiyegbami area 1 line 1 using 3D Stacked Column
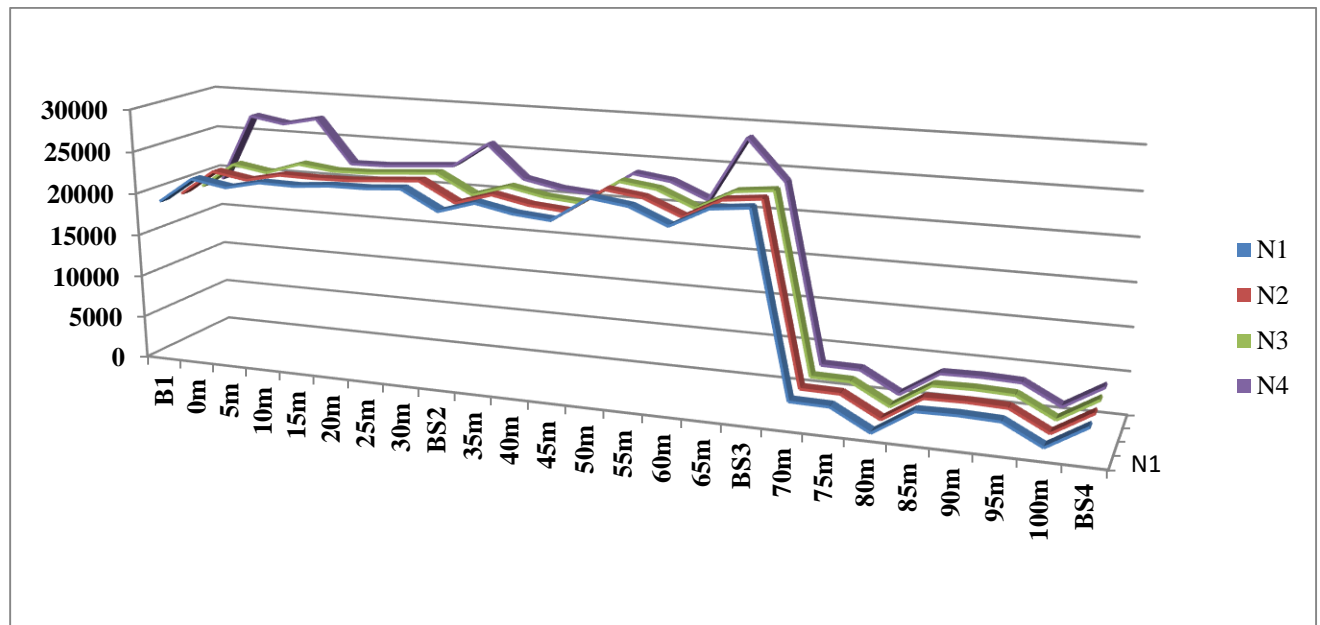
Figure 4.1b: Level of gravity changes in Aiyegbami 1 line 1 using 3D lines
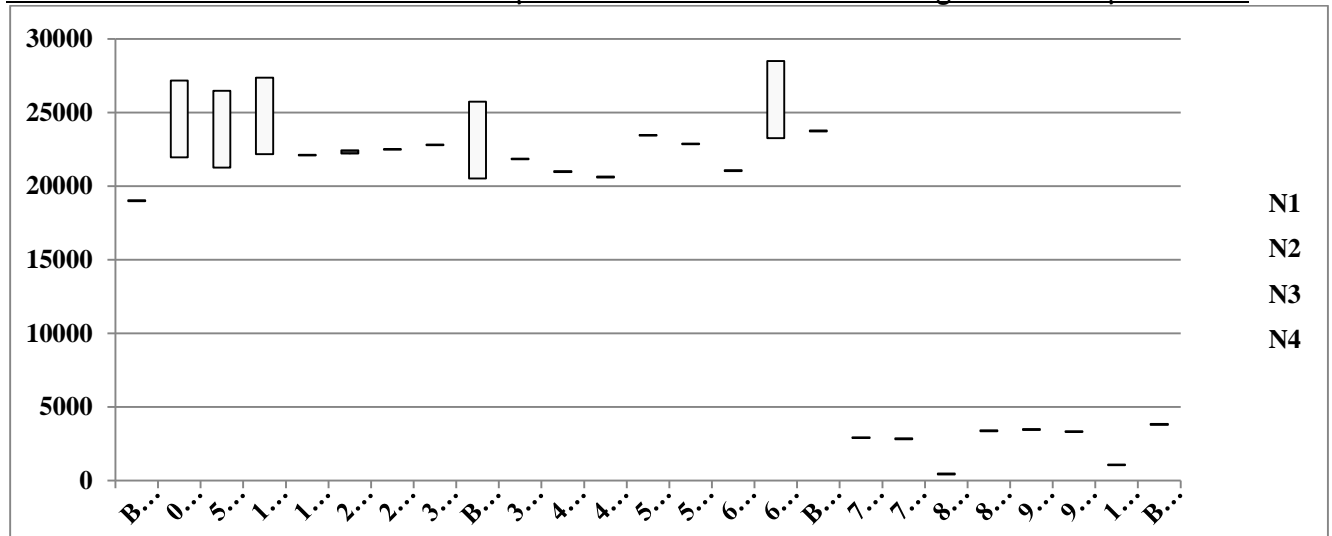
Figure 4.1c: High –Low close Description of gravity changes in Aiyegbami Area 1 in line1

4.1.2 Bouguer, Regional and Residual Anomaly in Traverse 1

The gravity profile along the traverse 1 is shown in Figure 4.1 - 4.3. A total length of 100 m with station spacing of 5 m was investigated. The bouguer anomaly data is plotted as profile and displayed in Figure 4.4a. Figure 4.4b is the regional-residual separation profile with a trend line representing the regional gravity field, and Figure 4.4c is the graph of the residual gravity profile showing the effect of the near-surface geology. The residual profile is interpreted for any gravity anomaly. From the residual anomaly plot, the profile shows major anomalous regions which occurred at lateral distance between 92 to100 m having gravity value of -800000. This anomalous zone is indicative of very low-density body that could lead to road failure within the study area.
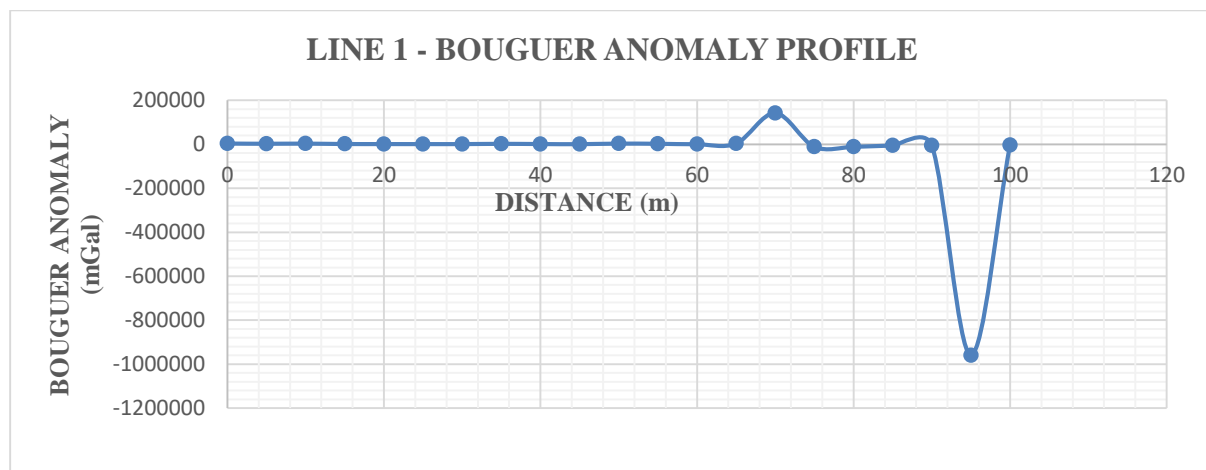
Figure 4.2a: Bouguer Anomaly Profile along Traverse 1
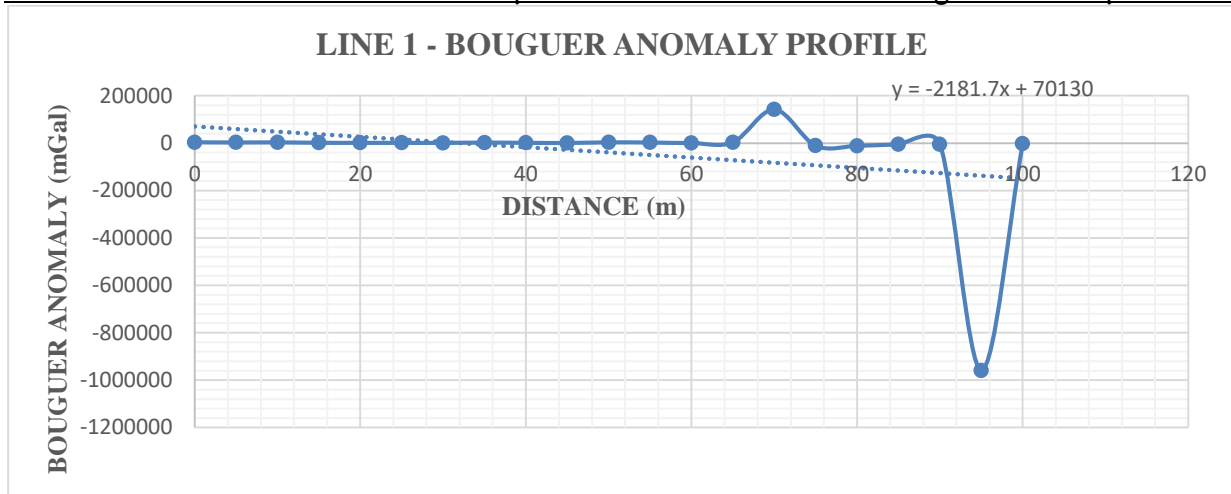
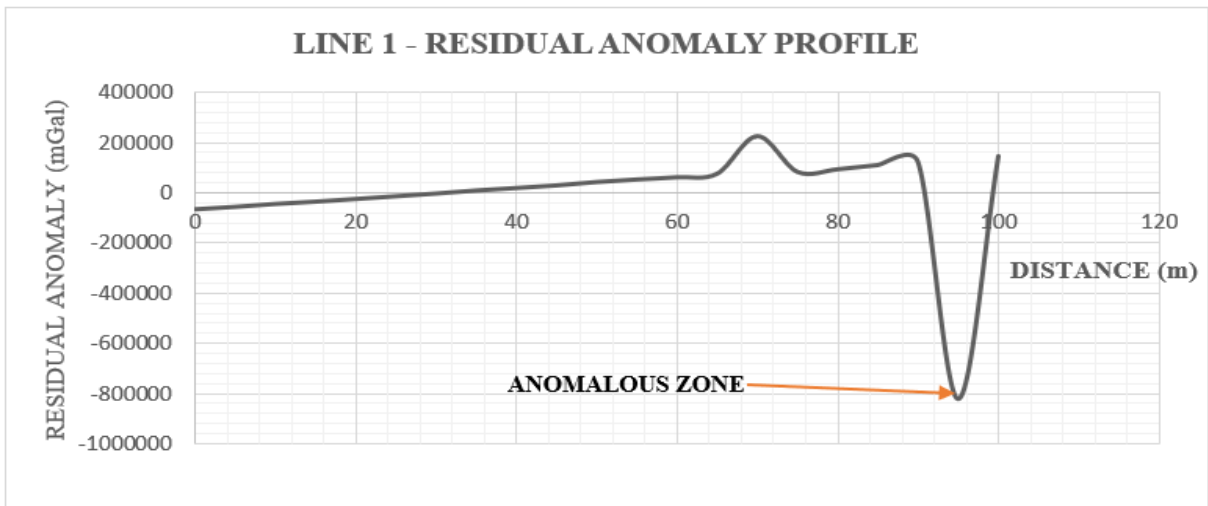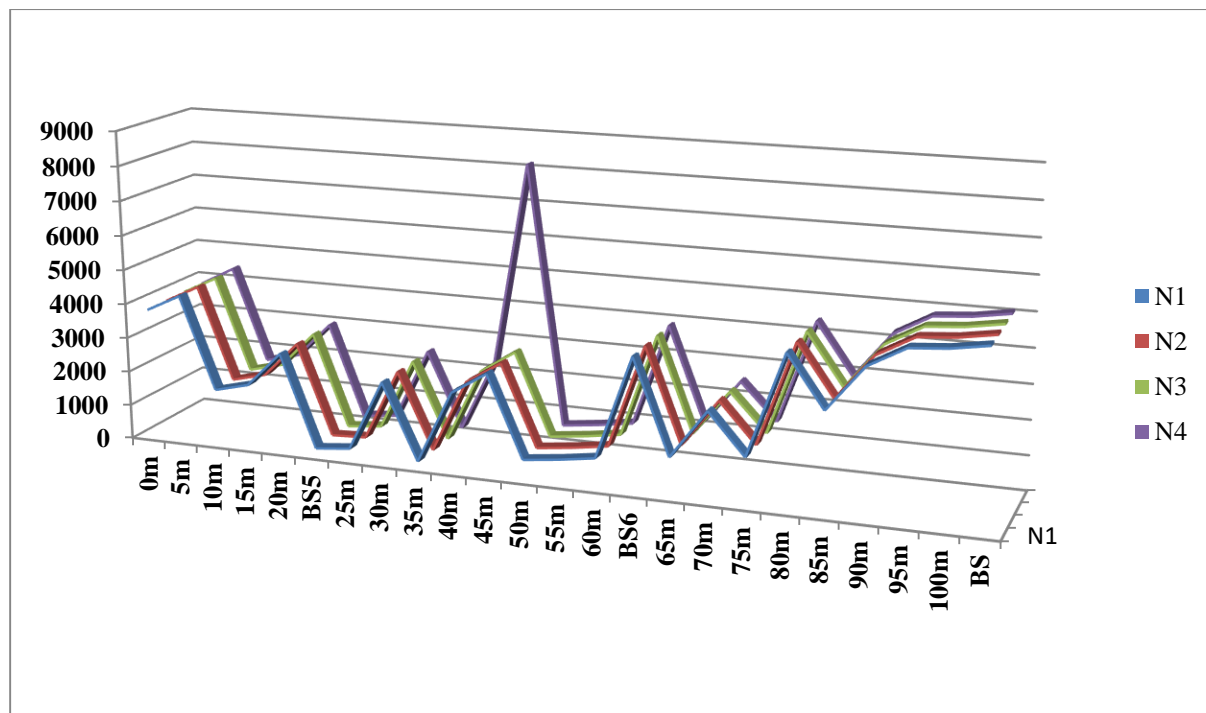Figure 4.2b: Regional - Residual Anomaly Profile along Traverse 1

Figure 4.2c: Residual Anomaly Profile along Traverse 1

Description of Gravity Variation in Traverse 1
The variation in gravity values were observed and interpreted using 3D Stacked Column, using 3D lines, High –Low close Description as respectively displayed in figure 4.3a, 4.3b and 4.3c for traverse line 1.
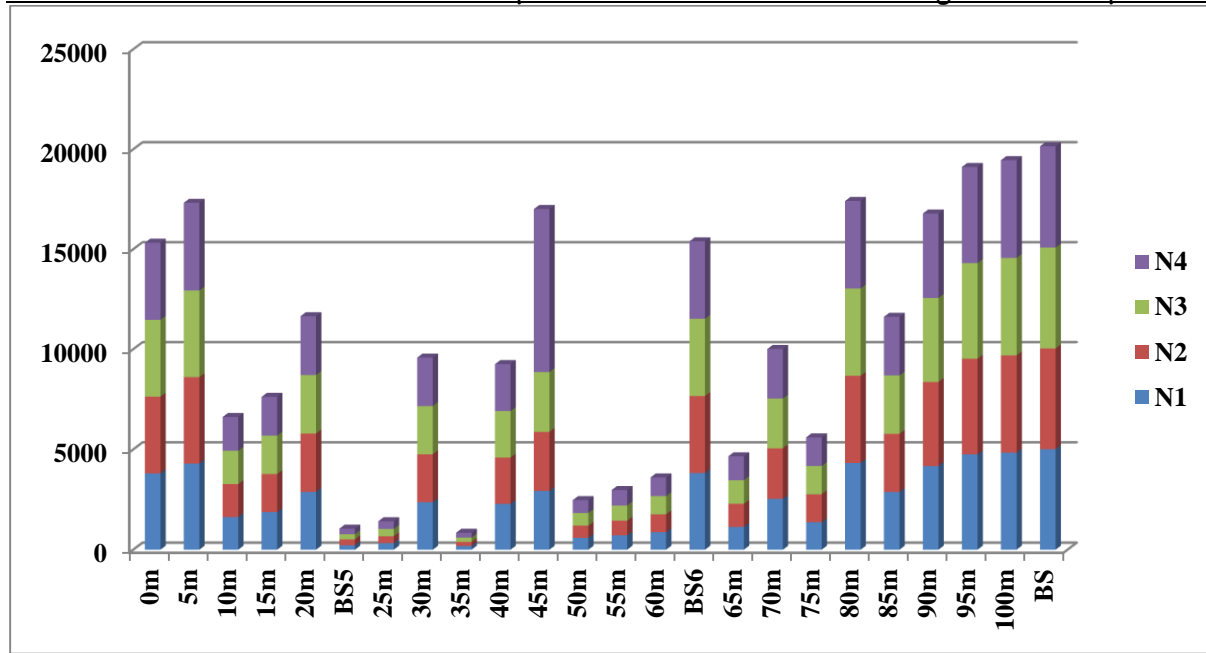
Figure 4.3a: Distribution of gravity changes using 3D Stacked Column in Aiyegbami area 1 line 2

Figure 4.3b: Level of gravity changes in Aiyegbami area1 line 2 using 3D lines
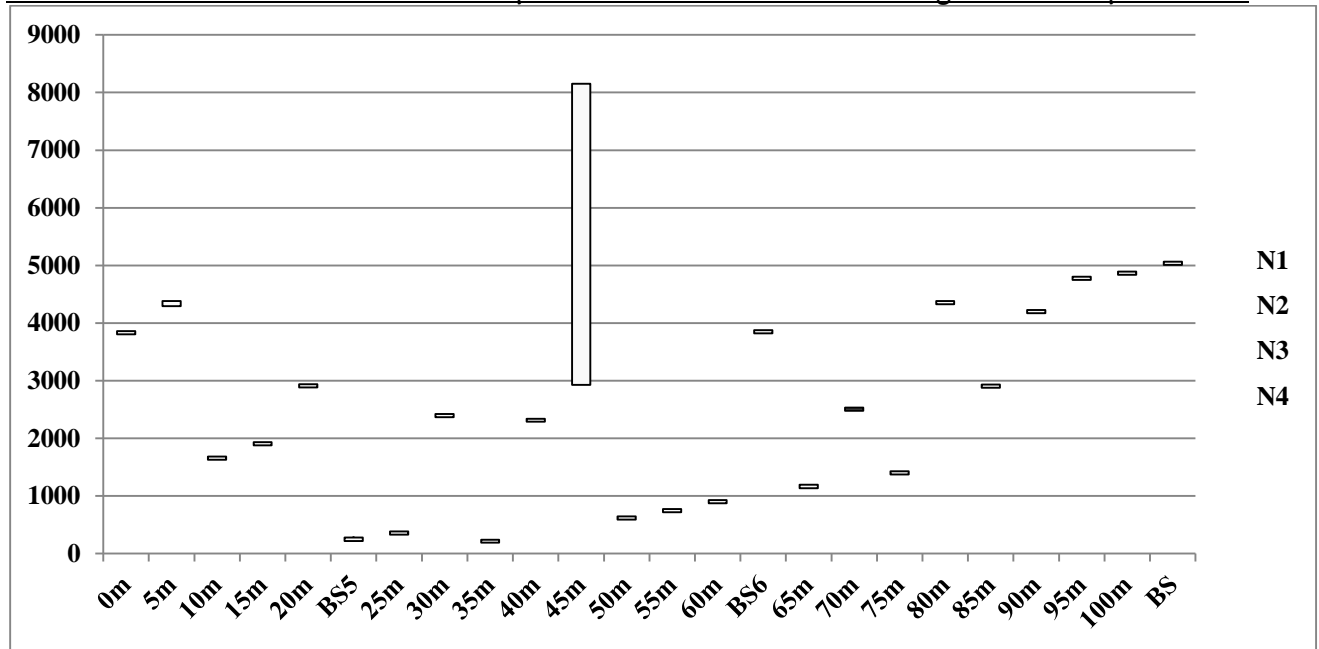
Figure 4.3c: High –Low close Description of gravity changes in Aiyegbami area 1 line 2

Bouguer, Regional and Residual Anomaly Profile in Traverse 2

The gravity profile along the traverse is shown in Figure 4.4a to 4.4c. A total length of 100 m with station spacing of 5 m was investigated. The bouguer anomaly data is plotted as profile and displayed in Figure 4.4a, 4.4b and 4.4c. Figure 4.4b is the regional residual separation profile with a trend line representing the regional gravity field, and Figure 4.4c is the graph of the residual gravity profile showing the effect of the near-surface geology. The residual profile is interpreted for any gravity anomaly. From the residual anomaly plot, the profile shows high and low anomalous regions which occurred at lateral distance between 0 to20 m and 24 to 64 m having gravity value of 4400 and -6000 mGal respectively. The low-density anomalous zone could pose a threat to the construction of road failure within the study area.
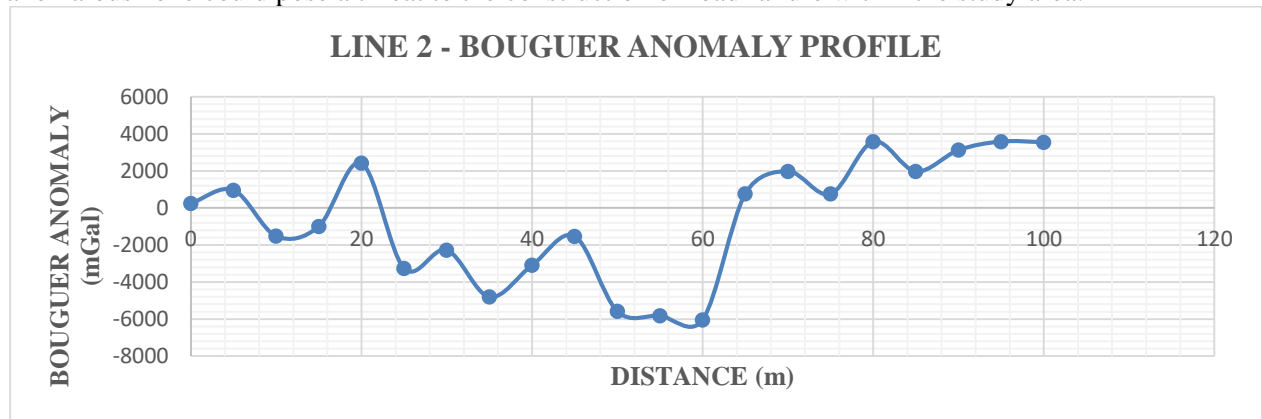

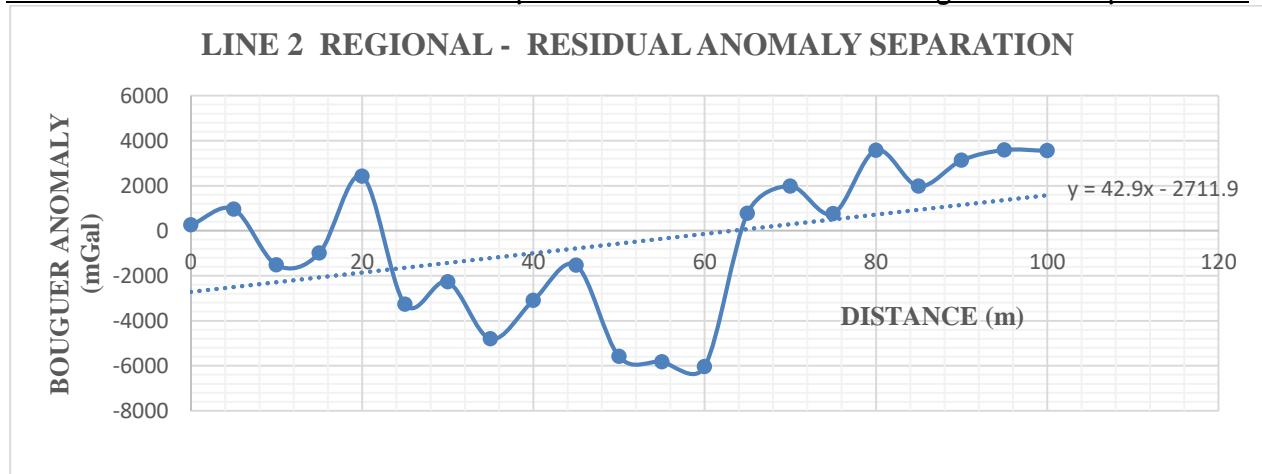Figure 4.4a: Bouguer Anomaly Profile along Traverse 2

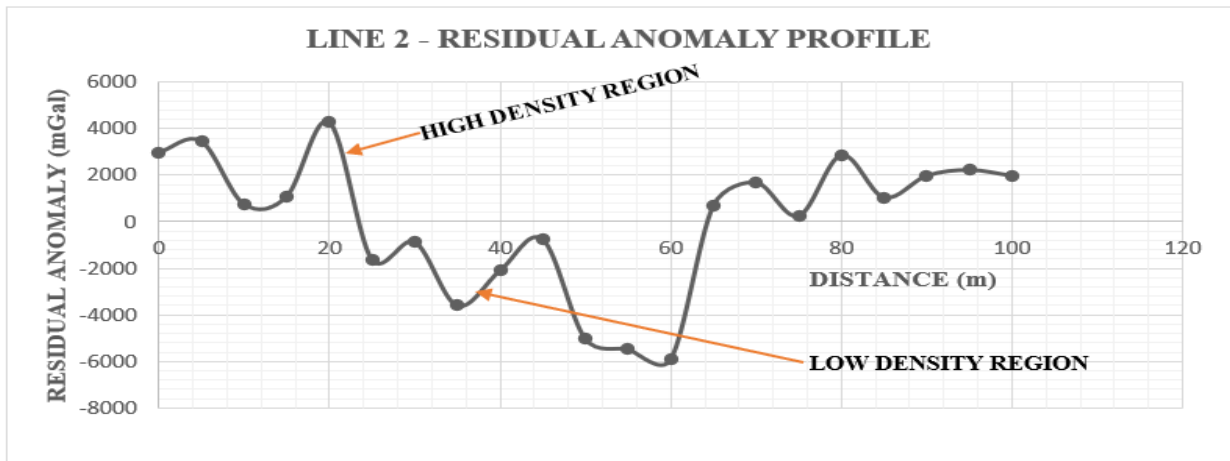Figure 4.4b: Regional - Residual Anomaly Profile along Traverse 2

Figure 4.4c: Residual Anomaly Profile along Traverse 2

CONCLUSION

Gravity method is a geophysical technique used to investigate sub- surface features by measuring variations in the earth gravitational field. The primary objective of gravity investigation is to identify sub-surface anomalies or geological structures such as mineral deposits, faults and tectonics structures using gravity data. CG-5 Autograv meter was used to measure the gravity variation at the location. A base station was established to serve as references due to variations in the earth's gravitational field and to make correction for drift. Two traverses were undertaken in the study area. Traverse 1 showed the residual anomaly plot profile where the major anomalous regions occurred at lateral distance between 92 to 100m having gravity value of -800000 mGal. This anomalous zone is indicative of very low-density body that could lead to road failure within the study area. Also, in traverse 2, the residual anomaly plot profile shows principally high

and low anomalous regions which occurred at lateral distance between 0 to 20m and 24m to 64m having gravity value of 4400 and -6000 mGal respectively. The identified low density anomalous zones in the identified regions could pose a threat to the construction of road within the study area because the gravity anomaly investigation showed that the materials are of low strength which can be improved when subjected to stabilization measures. The implication is that the residual soils within the subsurface of the studied area have low density. The subsurface materials cannot be used as construction materials except the materials are well compacted and stabilized appropriately in order for void spaces in the soil to be removed; these will intermittently reduce the permeability and increase the strength of the soil materials. It is therefore recommended that the subsurface materials be subjected to compaction and subsequent stabilization process under a standard geotechnical measures in order for it to give rise to the required strength that will withstand the impact of load and impede the inflow of water in the area (Olofinyo et al., 2019).

REFERENCES

Adeyemi, G.O (1995). The Influence of Parent Rock Factor on Some Engineering Index Properties of Three Residual Lateritic Soils in Southwestern Nigeria. Bull Int. Assoc. Eng. Geol. 52: 3-8.

Abubakar, A. M., and Likkason, B. K. (2022). Application of potential field gravity method in characterizing regional trends of the Earth's sequence system over the Sokoto Basin, NW, Nigeria. *Journal of Applied Geophysics, 206*, 104438

Adejuwon, S. A., Ojo, J. A., Akinpelu, J. A., and Oladipo, S. A. (2019). Ground gravity survey of 1:250,000 Sheet 61 (Akure), Southwestern Nigeria, underlain mainly by the Basement Complex rocks. *Journal of Geophysics and Engineering, 16*(3), 550-565.

Ajayi, T. A., & Adekoya, J. A. (2012). Gravity and magnetic survey of Ilesha area, southwestern Nigeria. *Journal of Geology and Mining Research, 4*(5), 111-120.

Alexander W.S and Maxwell J. (1996). Controlling Shrinkage Cracking from expansive Clay sub-grade. In: Feancken L.B., Molenaar A.A (Eds) Reflective Cracking in Pavements. 2nd Edition. E&FN Spon, London. pp. 64−71.

Akpan, O (2005). Relationship between road pavement failures, engineering indices and underlying geology in a tropical environment. Global Journal of Geoscience. 3(2): 99-108.

Azuwike, C. P., Akinluyi, F. O., & Aribo, F. J. (2020). Determination of crustal thickness within Northern Bida Basin, North Central Nigeria, using gravity data. *Geophysical Journal International, 223*(1), 429-443.

Barber, W., and Jones, G. P. (1965). The geology and hydrology of the Chad Basin. *Journal of African Earth Sciences, 1*(3), 67-82.

Black, R. (1980). The geology of Nigeria. *Journal of African Earth Sciences, 1*(2), 125-134.

Burke, K., Dewey, J. F., and Williams, J. R. (1971). The tectonic evolution of the Dahomey Basin. *Journal of the Geological Society of London, 127*(1), 125-143.

Dada, S. S. (2006). Geology of Nigeria and its mineral resources. *Geosciences Research, 3*(1), 10-20.

Enu, A. (1985). Sedimentology of the Afowo Formation, southwestern Nigeria. *Sedimentary Geology, 41*(4), 209-221.

Fotze, D. A., Mbida, S., and Nkoumbou, E. (2021). Structural interpretation of gravity data in Garoua, North Cameroon to delineate the structural framework of the area. *Geophysical Journal International, 226*(3), 1727-1742.

Gandu, J. S., Olayinka, A. I., and Fadairo, S. (1986). Granitoid plutons in Nigeria: A review. *Geological Magazine, 123*(5), 525-533.

Gupta, B.I., and Gupta, A (2003). Roads, railways, bridges, tunnel and harbor dock engineering. 5th Edn. Standard Publishers Distributors, Nai Sarak, New Delhi.

Ighodalo, C.A (2009). Transport Infrastructure and Economic Growth in Nigeria. Revised Paper Submitted For Presentation at the First International Conference on Transport Infrastructure (ICTI, 2008), Beijing, China. April 24-26. 2008

Igwe, O. O., Obi, J. O., and Eze, C. A. (2018). Investigation of Nsukka area, South-Eastern Nigeria for mineral exploration using gravity method. *International Journal of Earth Sciences and Engineering, 11*(2), 256-269.

Jegede, G (1997). Highway Pavement Failure Induced by Soil Properties along the F209 Highway at Omuoke, South-Western Nigeria. Nig. Journ. of Sci. pp. 4.

Klemme, H. D. (1975). The Dahomey Basin: Geology and exploration. *Petroleum Exploration Society of Australia Journal, 18*, 1-15.

Layade, J. A., Akinlua, A. O., and Olasunkanmi, A. T. (2020). Ground-based gravimetric survey for the detection and depth mapping of subsurface geological features of Ilesha, Southwest Nigeria. *Journal of African Earth Sciences, 164*, 104248.

Lowrie, W. (2007). *Fundamentals of geophysics* (2nd ed.). Cambridge University Press.

Lowrie, W. (2011). A Student's Guide to Geophysical Equations. Institute of Geophysics. Swiss Federal Institute of Technology Zurich Switzerland. Cambridge University Press. www.cambridge.org/9781107005846

Meshida, E.A (2006). Highway failure over talk-tremolite schist terrain: a case study of Ife to Ilesha Highway, Southwestern Nigeria. Bull Eng. Geo and Environment. 65: 457-461. https://doi.org/10.1007/s10064-005-0037-7

Nwoakoala, H.O., Amadi, A.N., Ushie F.A., Warmate, T (2014). Determination of Subsurface Geotechnical Properties for Foundation Design and Construction in Akenfa Community, Bayelsa State Nigeria. American Journal of Civil Engineering. Arch 2(4): 130−135

Obaje, N. G. (2009). *Geology and mineral resources of Nigeria*. Springer.

Okpoli, C. G., Okoye, N. L., and Nwachukwu, J. C. (2019). Gravity data interpretation for subsurface litho-structural delineation: A case study of the Benue Trough, Nigeria. *International Journal of Physical Sciences, 14*(2), 45-56.

Okpoli, O. D., and Akingboye, A. A. (2019). Application of high-resolution gravity data for litho-structural and depth characterization around Igabi area, Northwestern Nigeria. *Journal of African Earth Sciences, 156*, 67-82.

Ogezi, A. E. (1977). Geochronology of the schist belts in Nigeria. *Geochimica et Cosmochimica Acta, 41*(10), 1387-1395.

Ojo, J. A., and Olorunfemi, M. O. (2007). Gravity and magnetic investigations of the Ibadan area, southwestern Nigeria. *Geophysics, 72*(5), B191-B198.

Oke S.A., Amadi A.N., Abalaka A.E., Nwosu J.E., Jibade, S.A (2009). Index and Compaction Properties of Laterite Deposits for Road Construction in Minna Area, Nigeria. Nigerian Journal of Cons.Tech Man 10(1-2): 28-35.

Olofinyo O.O; Olabode O.F., Fatoyinbo, I.O (2019). Engineering properties of Residual Soils in Part of Southwestern Nigeria: implication for road foundation. SN Applied Science. 1:507. https://doi.org/10.1007/s42452-019-0515-3

Omatsola, M. E., & Adegoke, O. S. (1981). Tectonic evolution of the Dahomey Basin. *Journal of African Earth Sciences, 1*(2), 103-110.

Rahaman, M. A. (1988). Recent advances in the study of the basement complex of Nigeria. In P. D. O. Chukwuma & O. A. Olade (Eds.), *Proceedings of the 1st Annual Conference of the Nigerian Mining and Geosciences Society* (pp. 45-56). Nigerian Mining and Geosciences Society.

Rahaman, M. A., and Ocan, F. (1978). The Migmatite-Gneiss Complex of Nigeria. *Geological Society of America Bulletin, 89*(12), 1690-1702. https://doi.org/10.1130/0016-7606(1978)89<1690>2.0.CO;2

Reynolds, J. M. (2011). An Introduction To Applied And Environmental Geophysics (2nd ed.). *Wiley-Blackwell.*

Salami B.M., Falebita, D.E., Fatoba, O.J., Ajala, M.O. (2012). Integrated Geophysical and Geotechnical Investigation of a Bridge Site-a case study of Swampy/Creek Environment in SE Lagos, Nigeria. Ife Journal of Science. 14(1):75-82.

Telford, W. M., Geldart, L. P., and Sheriff, R. E. (1990). *Applied geophysics* (2nd ed.). Cambridge University Press.

Woakes, M., and Olayinka, A. I. (1987). A review of the geology of Nigeria. *Journal of African Earth Sciences, 6*(3), 143-158. https://doi.org/10.1016/0899-5362(87)90035-6